

---

# Bayesian Optimization for Noisy Black-box Functions: A Comparative Study Using BoTorch

---

CHEN Yao

Department of Data Science  
City University of Hong Kong  
ychen3353-c@my.cityu.edu.hk

CHEN Ziang

Department of Data Science  
City University of Hong Kong  
ziangchen9-c@my.cityu.edu.hk

## Abstract

Bayesian optimization offers an efficient approach for optimizing expensive-to-evaluate noisy black-box functions. Throughout its development, various mean functions, kernel functions, and acquisition functions have been employed to address various Bayesian optimization scenarios, with novel acquisition functions continually emerging. Recent advancements in PyTorch-based libraries like GPyTorch and BoTorch facilitate systematic comparisons of optimization performance across different acquisition functions. In this paper we employ five benchmark test functions (Ackley, Bohachevsky, Booth, Easom, Three-Hump Camel) as objectives to compare optimization effectiveness under combinations of three mean functions (Constant, Linear, Quadratic), three kernel functions (RBF, Matern(3/2), Matern(5/2)), and eight acquisition functions suitable for noisy single-objective optimization (qSR, qUCB, qLogNoisyEI, qPES, qMVE, qLBMVE, qKG, TS). Additionally, we present a BoTorch-based implementation framework for Bayesian optimization with discussions on critical implementation details. The code is available at <https://github.com/ZiangChen9/SDSC6002.git>.

## 1 Introduction

In many real-world optimization problems, particularly those characterized by expensive and noisy objective functions, the number of allowable function evaluations is often severely limited due to time, cost, or resource constraints. Traditional optimization methods may struggle in such settings, either requiring an impractically large number of evaluations or being overly sensitive to noise. Bayesian Optimization (BO) has emerged as a powerful framework to address these challenges. By constructing a probabilistic surrogate model of the objective function, BO enables efficient global optimization through informed sampling strategies that balance exploration and exploitation [Shahriari et al. \[2016\]](#).

A typical Bayesian Optimization procedure consists of the following steps:

1. A small set of initial input points is selected—usually via space-filling methods (such as Latin Hypercube Sampling or Sobol sequences) and the corresponding noisy objective function values are observed.
2. A probabilistic surrogate model, most commonly a Gaussian Process (GP), is fitted to the collected data, yielding a posterior distribution over the objective function.
3. An acquisition function is optimized to determine the next query point by leveraging both the predicted mean and uncertainty from the GP model.
4. The true (noisy) objective function is evaluated at the selected point, and the surrogate model is updated with the new observation.

5. Steps (2) to (4) are repeated iteratively until the predefined evaluation budget is exhausted.

This model-based optimization process is particularly well-suited for problems where each function evaluation is expensive and prone to stochasticity.

To facilitate the implementation and experimentation of Bayesian Optimization algorithms, the BoTorch library has been introduced as a modern, modular, and flexible platform. Built on top of PyTorch and seamlessly integrated with GPyTorch, BoTorch provides comprehensive support for defining and optimizing a wide range of surrogate models and acquisition functions. Notably, it offers a suite of advanced tools for modeling noisy observations, batch evaluations, and parallel optimization, making it well-suited for high-cost, noisy settings. However, despite its capabilities, BoTorch’s current documentation and usage examples remain limited, posing a potential barrier for researchers and practitioners seeking to explore its full potential.

In this paper, we present a systematic empirical study on the performance of eight Monte Carlo-based acquisition functions in noisy single-objective Bayesian optimization. Our evaluation covers 9 Gaussian Process configurations, formed by combining three types of prior mean functions (Constant, Linear, Quadratic) with three commonly used kernel functions (RBF, Matérn<sup>(3/2)</sup>, Matérn<sup>(5/2)</sup>). We benchmark these configurations on five representative test functions—Ackley, Bohachevsky, Booth, Easom, and Three-Hump Camel—chosen to reflect a variety of optimization landscapes including multi-modal, bowl-shaped, plate-shaped, rugged, and valley-shaped structures. The remainder of this paper is organized as follows:

- **Section 2** introduces the Gaussian Process surrogate modeling framework and the acquisition functions used in this paper.
- **Section 3** describes the experimental setup and evaluation protocol.
- **Section 4** presents the empirical results.
- **Section 5** offers a detailed discussion and interpretation of the findings.
- **Section 6** concludes the paper with key takeaways, limitations, and directions for future work.

## 2 Bayesian Optimization Framework

Bayesian Optimization (BO) is fundamentally built upon two closely coupled components: a probabilistic surrogate model, which approximates the unknown objective function, and an acquisition function, which guides the selection of future query points based on the surrogate’s posterior distribution. These two components form the backbone of the BO loop and jointly determine the sample efficiency and robustness of the optimization process.

in this paper, we adopt a **Gaussian Process (GP)** as the surrogate model due to its non-parametric nature and closed-form posterior inference, which make it particularly well-suited for modeling noisy and expensive black-box functions. The GP not only provides point estimates of the objective function but also quantifies predictive uncertainty, enabling a principled trade-off between exploration and exploitation.

The **acquisition function**, defined on top of the GP posterior, evaluates the utility of candidate points by scoring their potential to improve the objective or reduce uncertainty about its optimum. At each iteration, the next evaluation point is selected by maximizing the acquisition function over the input domain, after which the true (noisy) objective value is observed and incorporated into the model. This iterative mechanism gradually refines the surrogate and steers the optimization towards optimal regions.

The overall Bayesian optimization procedure adopted in this paper is summarized in **Figure 1** and detailed in **Algorithm 1**. The process begins with an initial design generated via a space-filling Sobol sequence, followed by repeated model fitting and acquisition optimization steps, until the evaluation budget is exhausted.

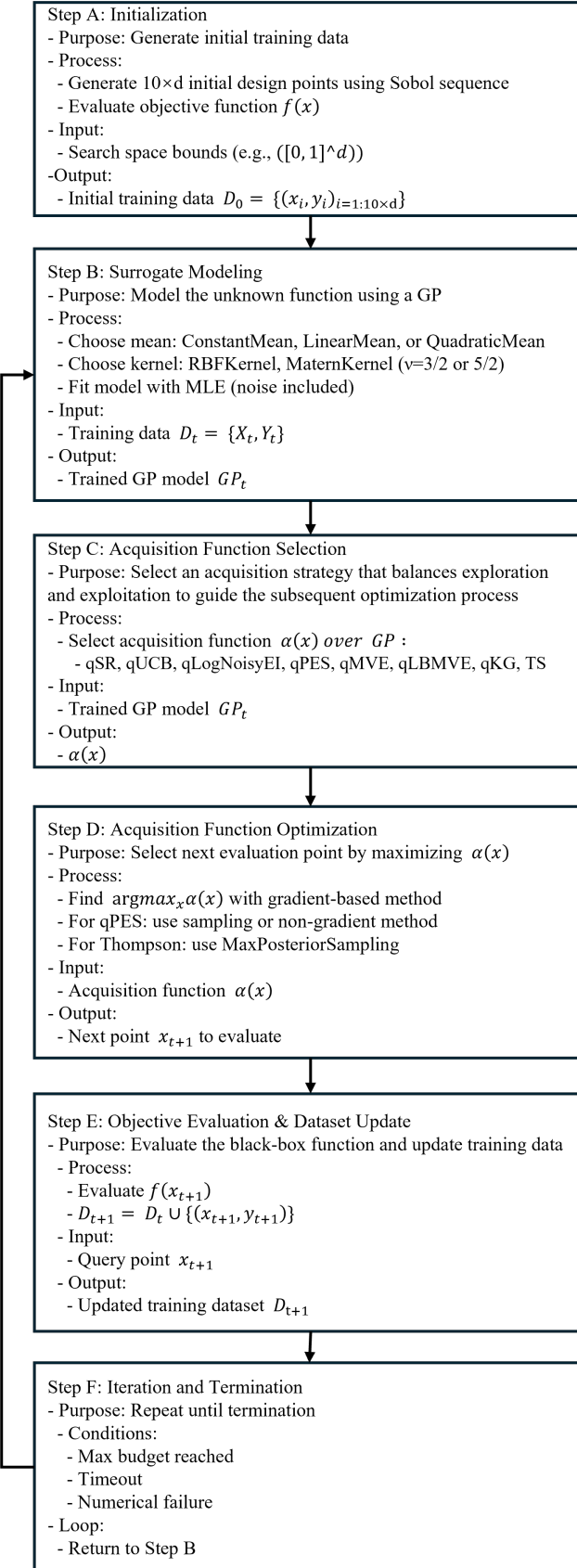


Figure 1: Bayesian Optimization Loop

---

**Algorithm 1** Bayesian Optimization with Gaussian Process Surrogate Model

---

```

1: Input: dimension  $d$ , budget, objective function  $f(\cdot)$ , noise  $\epsilon$ ,  $y(\cdot) = f(\cdot) + \epsilon$ 
2: Output: final dataset  $\mathcal{D}$ , estimated optimal solution  $\mathbf{x}^*$ 
3: Initialization:
4:   Generate  $10d$  initial points using Sobol sequence:  $\mathbf{X}_0 = \{\mathbf{x}_1, \mathbf{x}_2, \dots, \mathbf{x}_{10d}\}$ 
5:   Evaluate the objective function for each initial point:  $\mathbf{Y}_0 = \{y(\mathbf{x}_1), y(\mathbf{x}_2), \dots, y(\mathbf{x}_{10d})\}$ 
6:   Initialize the dataset:  $\mathcal{D}_0 = \{(\mathbf{x}_i, y_i) \mid i = 1, 2, \dots, 10d\}$ 
7: Construct Gaussian Process Surrogate Model:
8:   Select mean functions:
9:      $\mathcal{M} = \{\mu_{\text{Constant}}(\mathbf{x}), \mu_{\text{Linear}}(\mathbf{x}), \mu_{\text{Quadratic}}(\mathbf{x})\}$ 
10:  Select covariance functions:
11:     $\mathcal{K} = \{k_{\text{RBF}}(\mathbf{x}, \mathbf{x}'), k_{\text{Matérn}}(3/2)(\mathbf{x}, \mathbf{x}'), k_{\text{Matérn}}(5/2)(\mathbf{x}, \mathbf{x}')\}$ 
12:  Estimate parameters via maximum likelihood estimation on  $\mathcal{D}$ 
13:  Fit GP surrogate model  $GP(\mathcal{D})$ 
14: Select Acquisition Functions:
15:   Acquisition Functions set:
16:      $\mathcal{A} = \{\alpha_{\text{qSR}}, \alpha_{\text{qUCB}}, \alpha_{\text{qLogNoisyEI}}, \alpha_{\text{qPES}}, \alpha_{\text{qMVE}}, \alpha_{\text{qLBMVE}}, \alpha_{\text{qKG}}, \alpha_{\text{TS}}\}$ 
17: while budget  $T$  not exhausted and not timed out and no numerical instability do
18:   Score candidate points using  $\alpha(\cdot) \in \mathcal{A}$  based on current  $GP(\mathcal{D})$                                  $\triangleright$  Optimization Process
19:   Update the dataset:  $\mathcal{D}' = \mathcal{D} \cup \{(\mathbf{x}_{\text{new}}, y_{\text{new}})\}$                                  $\triangleright$  Scoring
20:   Refit  $GP(\mathcal{D}')$                                  $\triangleright$  Acquisition function Optimization
21:   if  $\alpha(\cdot) = \alpha_{\text{TS}}$ 
22:     See Algorithm 2
23:   else if  $\alpha(\cdot) \neq \alpha_{\text{qPES}}$ 
24:     Use gradient-based optimization to find  $\mathbf{x}_{\text{new}} = \arg \max \alpha(\mathbf{x})$ 
25:   else
26:     Use gradient-free optimization to find  $\mathbf{x}_{\text{new}} = \arg \max \alpha(\mathbf{x})$ 
27:   end if
28:   Evaluate the objective function at the new point:  $y_{\text{new}} = f(\mathbf{x}_{\text{new}}) + \epsilon$ 
29:   Update the dataset:  $\mathcal{D}' = \mathcal{D} \cup \{(\mathbf{x}_{\text{new}}, y_{\text{new}})\}$ 
30:   Refit  $GP(\mathcal{D}')$ 
31: end while
32: Output Results:
33:   Find  $\mathbf{x}^* = \arg \min_{(\mathbf{x}, y) \in \mathcal{D}} y$ 
34:   Return  $f(\mathbf{x}^*)$  and  $\mathcal{D}$ 

```

---

## 2.1 Gaussian Process Surrogate Model

in this paper, we employ a **noisy Gaussian Process (GP) surrogate model** for Bayesian optimization. A GP is a nonparametric model defined by a prior mean function  $\mu_0(\mathbf{x})$  and a positive semi-definite covariance function  $k(\mathbf{x}, \mathbf{x}')$ . Given a set of input-output pairs  $\mathcal{D}_n = \{(\mathbf{x}_i, y_i)\}_{i=1}^n$ , the GP assumes that the latent function values  $\mathbf{f} = [f(\mathbf{x}_1), \dots, f(\mathbf{x}_n)]^\top$  and the observations  $\mathbf{y} = \mathbf{f} + \boldsymbol{\epsilon}$  are jointly Gaussian:

$$\mathbf{f} | \mathbf{X}_{1:n} \sim \mathcal{N}(\mathbf{m}, \mathbf{K}), \quad \mathbf{y} | \mathbf{f} \sim \mathcal{N}(\mathbf{f}, \sigma^2 \mathbf{I}) \quad (1)$$

where:

- $\mathbf{X}_{1:n} = \{\mathbf{x}_1, \dots, \mathbf{x}_n\}$  is the set of training input points
- $\mathbf{m} = [\mu_0(\mathbf{x}_1), \dots, \mu_0(\mathbf{x}_n)]^\top$  is the prior mean vector
- $\mathbf{K}$  is the covariance matrix with elements  $K_{ij} = k(\mathbf{x}_i, \mathbf{x}_j)$
- $\boldsymbol{\epsilon} \sim \mathcal{N}(0, \sigma^2 \mathbf{I})$  represents the observation noise
- $\sigma^2$  is the observation noise variance

The **posterior mean** and **variance** of the function value at a test point  $\mathbf{x}$  are given by:

$$\mu_n(\mathbf{x}) = \mu_0(\mathbf{x}) + \mathbf{k}(\mathbf{x})^\top (\mathbf{K} + \sigma^2 \mathbf{I})^{-1} (\mathbf{y} - \mathbf{m}) \quad (2)$$

$$\sigma_n^2(\mathbf{x}) = k(\mathbf{x}, \mathbf{x}) - \mathbf{k}(\mathbf{x})^\top (\mathbf{K} + \sigma^2 \mathbf{I})^{-1} \mathbf{k}(\mathbf{x}) \quad (3)$$

Here,  $\mathbf{k}(\mathbf{x}) = [k(\mathbf{x}, \mathbf{x}_1), \dots, k(\mathbf{x}, \mathbf{x}_n)]^\top$  is the vector of covariances between  $\mathbf{x}$  and the training inputs.

The **prior mean function**  $\mu_0(\mathbf{x})$  in our experiments is selected from:

- **Constant mean:**  $\mu_0(\mathbf{x}) = \mu_0$
- **Linear mean:**  $\mu_0(\mathbf{x}) = \mathbf{w}^\top \mathbf{x} + b$
- **Quadratic mean:**  $\mu_0(\mathbf{x}) = \mathbf{x}^\top \mathbf{A} \mathbf{x} + \mathbf{w}^\top \mathbf{x} + b$

We also experiment with three different covariance functions:

- **Radial Basis Function (RBF) kernel:**

$$k(\mathbf{x}, \mathbf{x}') = \theta_0^2 \exp\left(-\frac{1}{2}r^2\right)$$

- **Matérn kernel ( $\nu = 3/2$ ):**

$$k(\mathbf{x}, \mathbf{x}') = \theta_0^2 \left(1 + \sqrt{3}r\right) \exp(-\sqrt{3}r)$$

- **Matérn kernel ( $\nu = 5/2$ ):**

$$k(\mathbf{x}, \mathbf{x}') = \theta_0^2 \left(1 + \sqrt{5}r + \frac{5}{3}r^2\right) \exp(-\sqrt{5}r)$$

with  $r^2 = (\mathbf{x} - \mathbf{x}')^\top \mathbf{\Lambda} (\mathbf{x} - \mathbf{x}')$ , and  $\mathbf{\Lambda}$  is a diagonal matrix of inverse squared length-scales.

In these covariance functions:

- The hyperparameter  $\theta_0^2$  represents the signal variance
- $\mathbf{\Lambda} = \text{diag}(\lambda_1^{-2}, \dots, \lambda_d^{-2})$  contains length-scale parameters

To learn the hyperparameters  $\boldsymbol{\theta} = (\theta_0, \mu_0, \sigma^2, \lambda_1, \dots, \lambda_d)$ , we maximize the log marginal likelihood:

$$\log p(\mathbf{y} | \mathbf{X}_{1:n}, \boldsymbol{\theta}) = -\frac{1}{2}(\mathbf{y} - \mathbf{m})^\top (\mathbf{K} + \sigma^2 \mathbf{I})^{-1} (\mathbf{y} - \mathbf{m}) - \frac{1}{2} \log |\mathbf{K} + \sigma^2 \mathbf{I}| - \frac{n}{2} \log(2\pi) \quad (4)$$

## 2.2 Acquisition Functions in Bayesian Optimization

In Bayesian Optimization (BO), acquisition functions are critical for directing the search towards the global optimum of a black-box function. Given a probabilistic surrogate model—typically a Gaussian Process (GP)—the acquisition function evaluates candidate points based on their potential to improve upon the current best observation. It effectively balances *exploration* of uncertain regions and *exploitation* of areas with promising predictions. At each iteration, the point that maximizes the acquisition function is selected for evaluation, thereby driving the optimization process.

This study employs the BoTorch library, a flexible and modular framework built on PyTorch, to implement the BO process. BoTorch offers both **analytic** acquisition functions, which have closed-form expressions suitable for single-point evaluations (i.e.,  $q = 1$ ), and **(quasi-) Monte Carlo (MC)** acquisition functions, which approximate expectations via sampling and can handle more complex scenarios, such as batch evaluations ( $q > 1$ ) and noisy observations. Notably, MC-based acquisition functions in BoTorch typically begin with the prefix  $q$ , such as  $qExpectedImprovement$  or  $qUpperConfidenceBound$ , indicating support for evaluating multiple candidates simultaneously.

Although MC acquisition functions are often associated with batch evaluations, they are equally applicable and beneficial in single-point settings, especially when dealing with noisy objective functions. Analytic acquisition functions generally assume noise-free outputs, which can lead to biased decisions in the presence of stochasticity. In contrast, MC-based methods estimate acquisition values by integrating over the posterior distribution of the surrogate model, thereby capturing uncertainty introduced by observational noise. Furthermore, BoTorch enhances efficiency by leveraging techniques such as the **reparameterization trick**, **(quasi-) Monte Carlo sampling**, and **fixed base samples**, which allow the acquisition functions to be optimized using deterministic and fast gradient-based methods like L-BFGS. These advantages make MC-based acquisition functions not only more robust under noise but also computationally efficient in practice.

Consequently, this paper focuses on MC-based acquisition functions within the BoTorch framework for optimizing noisy single-objective functions using GP surrogates. This choice leverages their robustness to noise and computational efficiency, even in the absence of batch evaluations.

### 2.2.1 qSimpleRegret(qSR)

The qSimpleRegret (qSR) acquisition function evaluates the expected immediate reward of evaluating a candidate point set  $X = (x_1, \dots, x_q)$  by computing the expectation of the maximum posterior prediction from the Gaussian process (GP) surrogate model. Formally, it is defined as:

$$\alpha_{qSR}(X) = \mathbb{E}[\max Y], \quad Y \sim GP(X),$$

where  $Y$  represents posterior samples at  $X$ . Unlike improvement-based methods, qSR directly targets the *current best predicted value* rather than potential future gains, making it particularly suitable for the final recommendation phase in Bayesian optimization (BO) where the goal is to identify the optimal observed solution [Balandat et al. [2020]].

In BoTorch, qSR is implemented through quasi-Monte Carlo (QMC) sampling (e.g., SobolQMCNormalSampler) to approximate the expectation. The algorithm generates low-discrepancy samples from the GP posterior, computes the maximum value within each sample batch, and averages these maxima to estimate the simple regret. For constrained optimization, BoTorch enforces feasibility via ConstrainedMCOObjective, which adjusts negative objective values to ensure non-negativity. In practice, the acquisition function is optimized using gradient-based methods (e.g., L-BFGS), with critical parameters including the sampler's sample size (e.g., 1,024 samples) and the number of optimization restarts (e.g., 20) to mitigate local optima. This approach balances computational efficiency with accurate regret estimation, aligning with scenarios requiring reliable final recommendations in noisy environments.

### 2.2.2 qUpperConfidenceBound(qUCB)

The qUpperConfidenceBound (qUCB) acquisition function extends the analytic Upper Confidence Bound (UCB) strategy to noisy and batch optimization settings via Monte Carlo (MC) sampling. Formally, it computes an optimistic bound on the objective function by evaluating the expectation:

$$\alpha_{qUCB}(X) = \mathbb{E} \left[ \max \left( \mu + |\tilde{Y} - \mu| \right) \right], \quad \tilde{Y} \sim \mathcal{N} \left( \mu, \beta \frac{\pi}{2} \Sigma \right),$$

where  $\mu$  and  $\Sigma$  are the posterior mean and covariance of the Gaussian process (GP) surrogate model at candidate points  $X$ , and  $\beta$  is a tunable hyperparameter controlling the exploration-exploitation trade-off. This reparameterization-based formulation, derived from [Wilson et al. [2017]], ensures theoretical guarantees for regret minimization while accommodating noisy evaluations.

In BoTorch, qUCB is implemented using quasi-Monte Carlo (QMC) sampling (e.g., SobolQMCNoMALSampler) to approximate the expectation. The algorithm generates perturbed samples  $\tilde{Y}$  from the GP posterior, scales deviations by  $\beta$ , and computes the maximum optimistic value for each sample. For constrained optimization, feasibility is enforced via ConstrainedMCOObjective, adjusting negative values to ensure numerical stability. In practice, the acquisition function is optimized with gradient-based methods (e.g., L-BFGS), leveraging parameters such as the sampler's sample size (e.g., 1024 samples) and exploration weight  $\beta$  (e.g.,  $\beta = 0.1$ ) to prioritize exploitation in noisy single-point evaluations ( $q = 1$ ). This approach balances computational efficiency with robust exploration, making qUCB suitable for scenarios requiring systematic trade-offs between model uncertainty and predicted performance.

### 2.2.3 qLogNoisyExpectedImprovement(qLogNoisyEI)

The `qLogNoisyExpectedImprovement` (`qLogNoisyEI`) acquisition function is a Monte Carlo-based method tailored for Bayesian optimization (BO) in noisy settings. Formally, it computes the logarithm of the expected improvement (EI) over a baseline dataset  $X_{\text{baseline}}$ , defined as:

$$\alpha_{qLogNoisyEI}(X) = \log \mathbb{E} [\max (\max Y - \max Y_{\text{baseline}}, 0)],$$

where  $Y$  and  $Y_{\text{baseline}}$  are posterior samples from the Gaussian process (GP) surrogate model at candidate points  $X$  and historical evaluations  $X_{\text{baseline}}$ , respectively. The logarithmic transformation addresses numerical instability in regions with near-zero improvement probabilities, ensuring robust gradient computation during optimization. Unlike analytic EI variants (e.g., `ExpectedImprovement`), which assume noise-free observations, `qLogNoisyEI` integrates over perturbed posterior samples (“fantasy” sampling) to explicitly model observational noise, making it suitable for stochastic objective functions.

In BoTorch, `qLogNoisyEI` is implemented via quasi-Monte Carlo (QMC) sampling, leveraging a `SobolQMCNormalSampler` to generate low-discrepancy samples from the GP posterior. Key parameters include  $X_{\text{baseline}}$  (historical data for improvement benchmarking) and the sampler’s sample size (e.g., 1,024 samples), which balance computational cost and approximation accuracy. For single-point evaluations ( $q = 1$ ), the acquisition function is optimized using gradient-based methods (e.g., L-BFGS), enabled by reparameterization and fixed base samples to transform stochasticity into deterministic gradients. This design ensures both noise robustness and computational efficiency, aligning with the requirements of optimizing costly-to-evaluate noisy functions.

### 2.2.4 qPredictiveEntropySearch (qPES)

The `qPredictiveEntropySearch` (`qPES`) acquisition function implements the Predictive Entropy Search (PES) strategy, which selects candidate points by maximizing the mutual information between the unknown optimizer and the function values observed at candidate locations. This acquisition function estimates the expected reduction in entropy over the distribution of the optimizer after observing new evaluations. It is particularly well-suited for single-objective problems where the goal is to reduce uncertainty about the location of the global minimizer. The mutual information is approximated using an expectation propagation (EP) algorithm, which allows for a tractable estimation of the conditional entropy without requiring analytic posterior computations.

In BoTorch, `qPES` is implemented for single-outcome Gaussian process (GP) models and requires a predefined set of sampled optimal inputs, which represent plausible global optima drawn from the posterior distribution. The acquisition value is then computed based on the expected information gain from observing function values at the candidate points. Due to the non-differentiable nature of the EP-based approximation, BoTorch recommends using finite-difference optimization techniques. Additionally, since the EP algorithm can be numerically unstable in rare cases, particularly with many EP factors, jitter terms are introduced during training and testing to mitigate such risks. In practice, `qPES` can yield negative acquisition values due to estimation variance, though this does not impact the correctness of the optimization process. The implementation used in this paper follows BoTorch’s recommendations and applies finite-difference optimization (`with_grad=False`) with typical settings such as 20 restarts and 50 raw samples. This approach provides a robust and principled strategy for information-driven search under uncertainty.

### 2.2.5 q.MaxValueEntropySearch (qMVE)

The `q.MaxValueEntropy` (`qMVE`) acquisition function implements the Max-value Entropy Search (MES) strategy, which selects candidate points by maximizing the mutual information between the unknown global maximum value  $y_*$  and the next evaluation point  $x$ . Following Wang and Jegelka [2017], the acquisition function is defined as:

$$\alpha_{qMVE}(x) = I(x, y_* | D_t) = H(p(y | D_t, x)) - \mathbb{E}_{y_*}[H(p(y | D_t, x, y_*))], \quad (5)$$

where  $D_t$  denotes the historical observations up to iteration  $t$ ,  $H(\cdot)$  is the entropy, and  $y_* = \max_{x \in \mathcal{X}} f(x)$ . This formulation quantifies the reduction in uncertainty about  $y_*$  after evaluating  $x$ ,

prioritizing points that maximally resolve ambiguity in the global maximum value [Wang and Jegelka \[2017\]](#).

In BoTorch, qMVE approximates the expectation through Monte Carlo (MC) sampling over a predefined candidate set  $\mathcal{C} \subset \mathcal{X}$ , which discretizes the domain to estimate the distribution of  $y_*$ . The implementation requires a dense candidate set (e.g., 10,000 points generated via Sobol sequences scaled to the feasible bounds. Posterior samples from the GP are used to compute entropy reduction via kernel density estimation (KDE). For single-point evaluations ( $q = 1$ ), the acquisition function is optimized using gradient-based methods, with critical parameters including the candidate set size (e.g.,  $|\mathcal{C}| = 10,000$ ) and the number of optimization restarts (e.g., 20) to avoid local optima. This approach balances computational tractability with accurate entropy estimation, making qMES particularly effective in scenarios where resolving uncertainty about the global optimum is critical, such as noisy or multi-modal optimization tasks.

### 2.2.6 qLowerBoundMaxValueEntropy (qLBMVE)

The qLowerBoundMaxValueEntropy (qLBMVE) acquisition function, proposed in the General-purpose Information-Based Bayesian Optimization (GIBBON) framework [Moss et al. \[2021\]](#), offers a computationally efficient approximation of the mutual information between the unknown global maximum value and candidate input points. Rather than evaluating the full mutual information, which is often computationally prohibitive, qLB-MES computes a lower bound on this quantity by estimating the information gain through discrete maximum value sampling. This formulation retains the core entropy reduction objective of Max-value Entropy Search (MES) while significantly reducing computational complexity by discretizing the distribution of potential maxima using a predefined candidate set. For a full derivation and explanation of the mathematical formulation, readers are referred to [Moss et al. \[2021\]](#).

In BoTorch, qLBMVE is implemented using quasi-Monte Carlo (QMC) sampling over a dense candidate set—for instance, 10,000 Sobol samples scaled to match the input bounds. These samples are used both to approximate the distribution of the maximum value and to support posterior sampling necessary for entropy estimation via kernel density methods. In the case of single-point selection ( $q = 1$ ), the acquisition function is typically optimized using gradient-based methods such as L-BFGS. Implementation parameters such as `candidate_set=10_000` ensure high-resolution entropy approximation, while settings like `num_restarts=20` help avoid poor local optima. This approach balances computational efficiency with principled exploration, making qLB-MES particularly well-suited for noisy optimization problems with limited evaluation budgets.

### 2.2.7 qKnowledgeGradient (qKG)

The qKnowledgeGradient (qKG) acquisition function implements the batch Knowledge Gradient strategy using a one-shot formulation. It selects candidate points by maximizing the expected utility gain after obtaining hypothetical observations at those points, thereby quantifying the value of information associated with evaluating a batch. This approach approximates the nested expectation over future outcomes by using a set of "fantasy" models—posterior samples drawn under simulated observations. The acquisition function evaluates how these fantasies affect the choice of future optima, either through the model posterior mean or Monte Carlo sampling. This formulation enables decision-theoretic optimization under uncertainty and generalizes to batch settings through joint optimization of candidates and fantasy decisions. A complete derivation of the one-shot qKG formulation is provided in [Balandat et al. \[2019\]](#), with earlier foundations in [Frazier et al. \[2008\]](#) and [Wu and Frazier \[2016\]](#).

In BoTorch, qKG is implemented using fantasy modeling for the outer expectation and allows differentiable or non-differentiable inner expectations. The user specifies the number of fantasy samples (e.g., 128), and all inputs—including real candidates and fantasy designs—are optimized jointly in a single acquisition call. In this paper, qKG is applied in the single-point setting ( $q = 1$ ), with the acquisition function optimized using 20 restarts and 50 raw samples. This configuration leverages the one-shot optimization framework with 128 fantasies, specified as `num_fantasies=128`. The resulting acquisition function provides a scalable approximation to the value of information, making qKG particularly effective for batch decision-making under noisy and high-cost evaluation conditions.

### 2.2.8 Thompson Sampling(TS)

The Thompson Sampling (TS) strategy is a randomized acquisition approach widely used in Bayesian optimization. Rather than computing acquisition scores for each candidate point, TS draws a single sample function from the posterior distribution of the surrogate model—typically a Gaussian process (GP)—and selects the input that maximizes this sample. Formally, TS replaces the unknown objective function with a single realization drawn from the GP posterior and queries the point where this sample attains its maximum. This sampling-based strategy inherently balances exploration and exploitation: regions with high predictive mean are likely to yield high values in the sample, while regions with high uncertainty have greater variance and thus a higher probability of being selected. Over multiple iterations, this randomness leads to robust and efficient exploration of the search space [THOMPSON \[1933\]](#).

In BoTorch, TS is implemented via the `MaxPosteriorSampling` class, which samples from the multivariate posterior over a predefined candidate set and returns the point with the highest sampled value. Since a sample from the GP posterior can only be defined over a finite number of points, TS requires a dense candidate set spanning the search space. This is typically generated using a Sobol sequence, which offers better coverage than uniform sampling. In this paper, a set of 5,000 Sobol points was generated and rescaled to match the input bounds. Sampling was performed without replacement to ensure diversity, and the selected point—corresponding to the maximum value in the posterior sample—was appended to the current dataset. This approach avoids explicit acquisition score computation and remains both simple and computationally efficient, particularly in noisy or high-dimensional settings. This strategy is simple, computationally efficient, and highly effective in noisy or high-dimensional optimization settings, where classical acquisition functions may become unstable or overly deterministic.

The Thompson sampling approach differs from other seven acquisition functions studied in this paper in that it does not optimize the acquisition function when selecting the next sampling point. Instead, it samples from the predictive distribution of the Gaussian process surrogate model to probabilistically select the next point, thereby balancing exploration and exploitation in a stochastic manner. The Bayesian optimization process using Thompson sampling is detailed in Algorithm 2

---

#### Algorithm 2 Thompson Sampling for Bayesian Optimization

---

```

1: Input: Gaussian Process surrogate model  $GP(\mathcal{D})$ 
2: Output: Next sampling point  $\mathbf{x}_{\text{new}}$ 
3: Initialization:
4:   Define the number of candidate points  $N_{\text{candidates}}$ 
5:   Generate a set of candidate points  $\mathbf{X}_{\text{candidates}} = \{\mathbf{x}_1, \mathbf{x}_2, \dots, \mathbf{x}_{N_{\text{candidates}}}\}$ 
6: Sampling Process:
7:   for each candidate point  $\mathbf{x}_i \in \mathbf{X}_{\text{candidates}}$  do
8:     Predict the mean  $\mu(\mathbf{x}_i)$  and variance  $\sigma^2(\mathbf{x}_i)$  using  $GP(\mathcal{D})$ 
9:     Get a sample from the predictive distribution:  $\mathcal{N}(\mu(\mathbf{x}_i), \sigma^2(\mathbf{x}_i))$ 
10:  end for
11: Selection:
12:   Select the candidate point with the highest sampled value:  $\mathbf{x}_{\text{new}} = \arg \max_{\mathbf{x}_i \in \mathbf{X}_{\text{candidates}}} y_i$ 
13: Output:
14:   Return the selected point  $\mathbf{x}_{\text{new}}$  as the next sampling point

```

---

## 3 Experiment

### 3.1 General Setup

All experiments were conducted on an Ubuntu server equipped with an NVIDIA L40 GPU (40GB VRAM), with CUDA acceleration enabled to support parallel computations in PyTorch. Detailed specifications of the experimental environment are provided in Table I. For each optimization task, we began with an initial design of 20 points sampled using a Sobol sequence. Subsequently, 80 Bayesian optimization iterations were performed, resulting in a total evaluation budget of 80 function evaluations beyond the initial design. To ensure statistically reliable results, each optimization

procedure was independently repeated 30 times, referred to as 30 replications. To maintain numerical precision and stability in Bayesian optimization, all computations were performed using float64 (double precision). The implications of using float32 (single precision) will be analyzed in Appendix C. In standard experimental configurations, we set the noise level  $\sigma$  to 0.5.

Table 1: Experimental Environment Configuration

Configuration	
OS	Ubuntu 22.04
Language	Python 3.12.9
Framework	Botorch 0.13.0
CPU	AMD EPYC 9654
GPU	NVIDIA L40(40G)

### 3.2 Special configuration

To accommodate the unique characteristics of certain benchmark functions and acquisition strategies, we implemented specific experimental configurations as detailed below.

The Easom function was assigned a lower noise level ( $\sigma = 0.2$ ) than other benchmarks ( $\sigma = 0.5$ ) due to its steep, narrow parabolic basin and sharp global optimum. This adjustment ensures a more appropriate signal-to-noise ratio, facilitating effective optimization.

The Bohachevsky and Booth functions were allocated only 10 iterations per replication because their shallow, parabolic landscapes (with gradient norms below 0.1 across 95% of the domain) allow reliable convergence within minimal iterations. This contrasts with multimodal functions like Ackley requiring 80 evaluations to escape local minima.

Regarding the qPES acquisition function, we disabled gradient computation (with `grad=False`) during optimization due to frequent numerical instabilities in its gradient calculation. These instabilities arise from the entropy-based objective's non-smoothness at sample boundaries and the Monte Carlo approximations of the posterior Hessian matrix, which can lead to ill-conditioned gradients.

The candidate set sizes were configured with 10,000 points for qMVE and qLBMVE, compared to 5,000 for qTS. This configuration was determined based on preliminary experiments, which indicated that for qMVE and qLBMVE, a candidate set size below 1,000 was insufficient to achieve satisfactory optimization performance. Increasing the candidate set size to 10,000 significantly improved the maximization of the acquisition function, while the increase in runtime was negligible. For qTS, a candidate set size of 5,000 was chosen to balance computational efficiency and optimization performance. The impact of candidate set size on optimization performance will be further analyzed in Appendix B.

These configurations are summarized in Table 2 and Table 3.

Table 2: Configuration of Benchmark Functions

Function	Noise Level	Repl.	Budget (Evaluations)	Searching Space (Optimal Value)
Ackley	0.5	30	80	$[-32.768, 32.768]^2$ (0.0)
Bohachevsky	0.5	30	10	$[-100.0, 100.0]^2$ (0.0)
Booth	0.5	30	10	$[-10.0, 10.0]^2$ (0.0)
Three-Hump Camel	0.5	30	80	$[-5.0, 5.0]^2$ (0.0)
Easom	0.2	30	80	$[-5.0, 5.0]^2$ (-1.0)

### 3.3 Evaluation

We conducted a comprehensive evaluation of eight acquisition functions across  $3 \times 3 = 9$  distinct Gaussian process configurations, representing all combinations of three kernel functions (RBF,

Table 3: Acquisition Function Configuration

Acquisition Function	with gradient	candidate set size	number of initial points
qSR	True	/	20
qUBC	True	/	20
qLogNoisyEI	True	/	20
qPES	False	/	20
qMVE	True	10000	20
qLBMVE	True	10000	20
qKG	True	/	20
TS	/	5000	20

Matérn-1.5, and Matérn-2.5) and three mean functions (constant, linear, and quadratic). This systematic assessment was performed on five benchmark objective functions, resulting in  $8 \times 9 \times 5 = 360$  distinct experimental conditions.

This extensive evaluation protocol supports statistically reliable conclusions by incorporating:

- Full factorial design covering major GP modeling choices
- Multiple random initializations (30 replications per condition)

## 4 Results

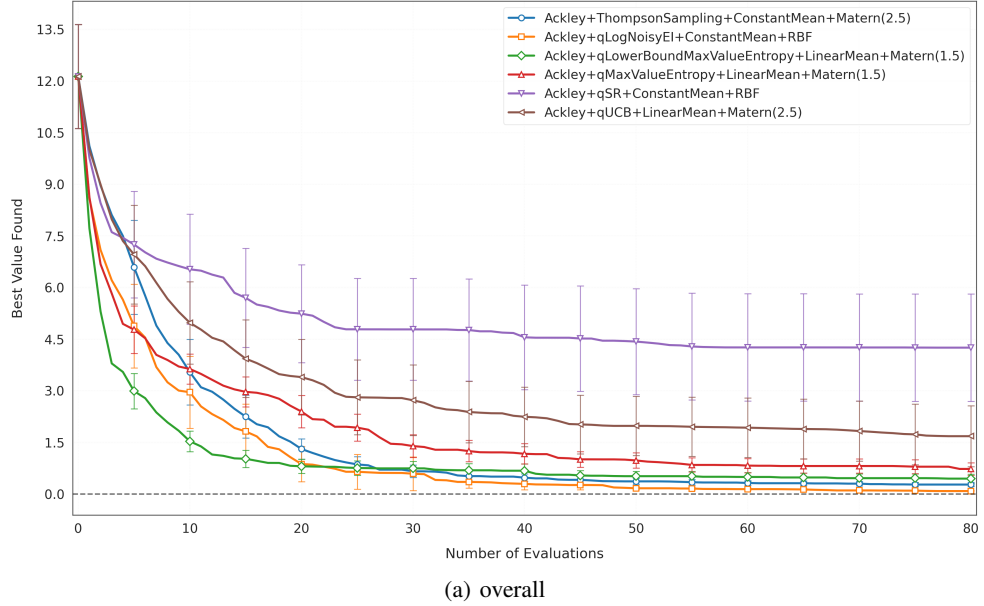
To evaluate the performance of different acquisition strategies under noisy single-objective Bayesian optimization, we conducted systematic experiments across five benchmark functions: Ackley, Bosphorus, Booth, Three-Hump Camel, and Easom. For each benchmark, eight acquisition functions were tested across 9 distinct Gaussian process (GP) configurations, defined by all combinations of three mean functions (constant, linear, quadratic) and three covariance kernels (RBF, Matérn-1.5, Matérn-2.5). Each configuration was evaluated over 30 replications, and the average best value found per evaluation was recorded. Error bars denote 95% confidence intervals calculated using the t-distribution.

For each acquisition function, performance curves corresponding to the 9 GP configurations were plotted (subfigures b–i). The configuration yielding the best overall performance was selected to represent that acquisition function. These best-performing curves across all acquisition functions were then compared in a summary plot (subfigure a), enabling high-level comparison among acquisition functions for each benchmark. The curve of the "overall" image is derived from the optimal combination of each acquisition function below. For example, in the case of Ackley's qLogNoisyEI, the combination of the constant mean and RBF kernel performs the best, so we select this combination as representation of qLogNoisyEI and incorporate it into the corresponding overall image for Ackley.

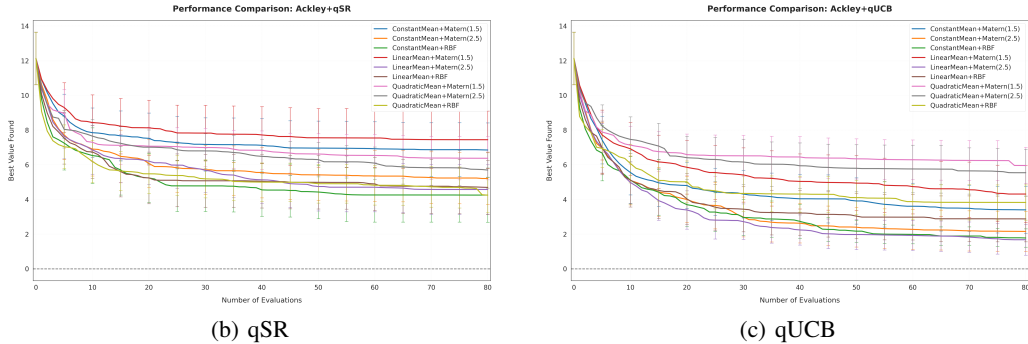
Due to occasional numerical instabilities or excessive runtime, not all acquisition-configuration combinations completed successfully. Consequently, the number of plotted curves may differ across figures. The table in last page (Table A1) presents the mean and standard deviation (calculated over 30 replications) of the best observed values at 25%, 50%, 75%, and 100% of the optimization budget (additional evaluations after initial sampling). The results cover 5 test functions evaluated with 8 acquisition functions, where each acquisition function was combined with 3 mean functions and 3 covariance functions (yielding 9 variants per acquisition function).

Figure 2: Ackley

**Performance Comparison: Ackley**

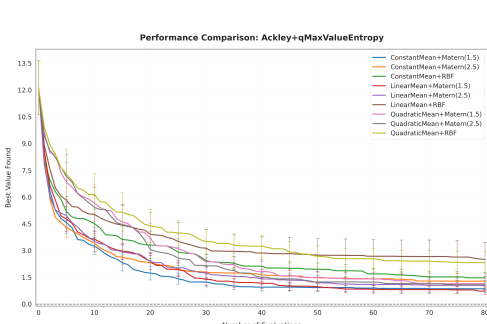


(a) overall



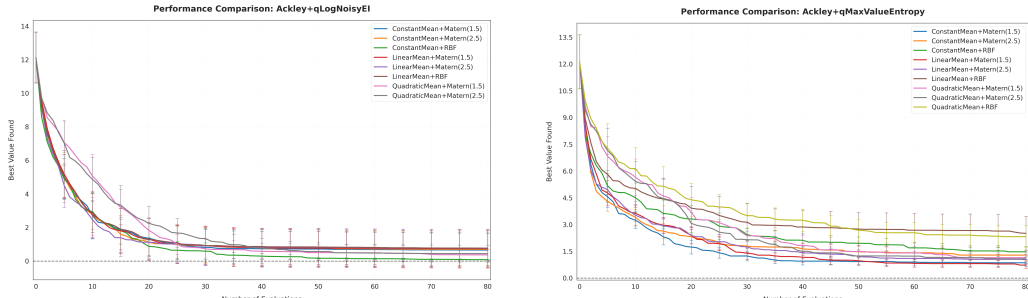
(b) qSR

Performance Comparison: Ackley+qUCB



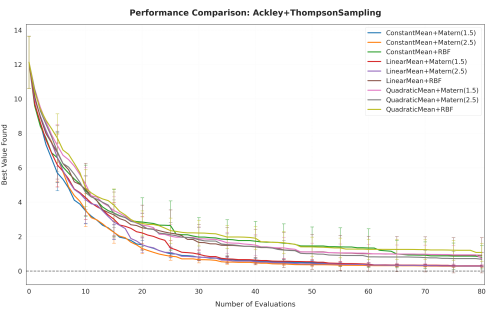
(d) qLogNoisyEI

Performance Comparison: Ackley+qMVE



(f) qLBMVE

(e) qMVE



(g) TS

Figure 3: Bohachevsky

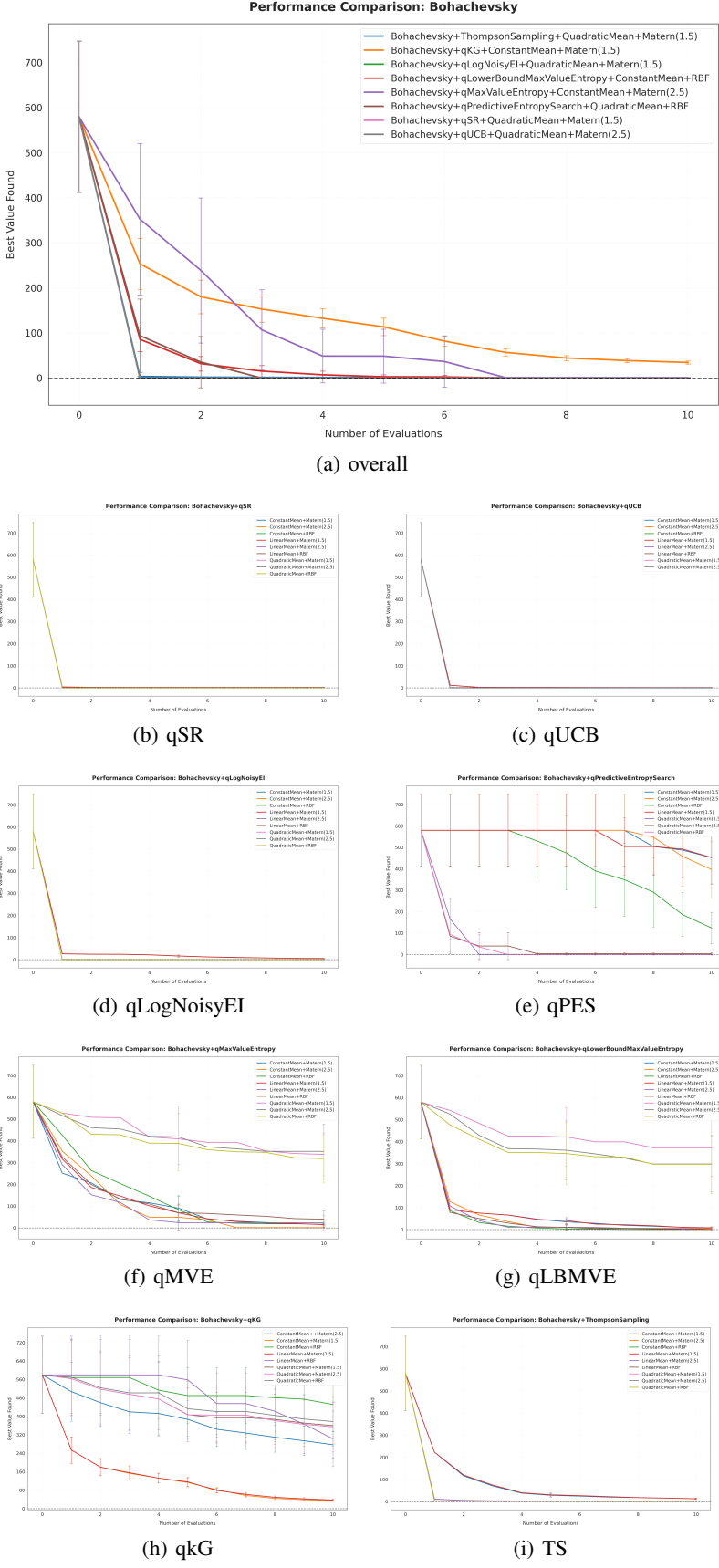


Figure 4: Booth

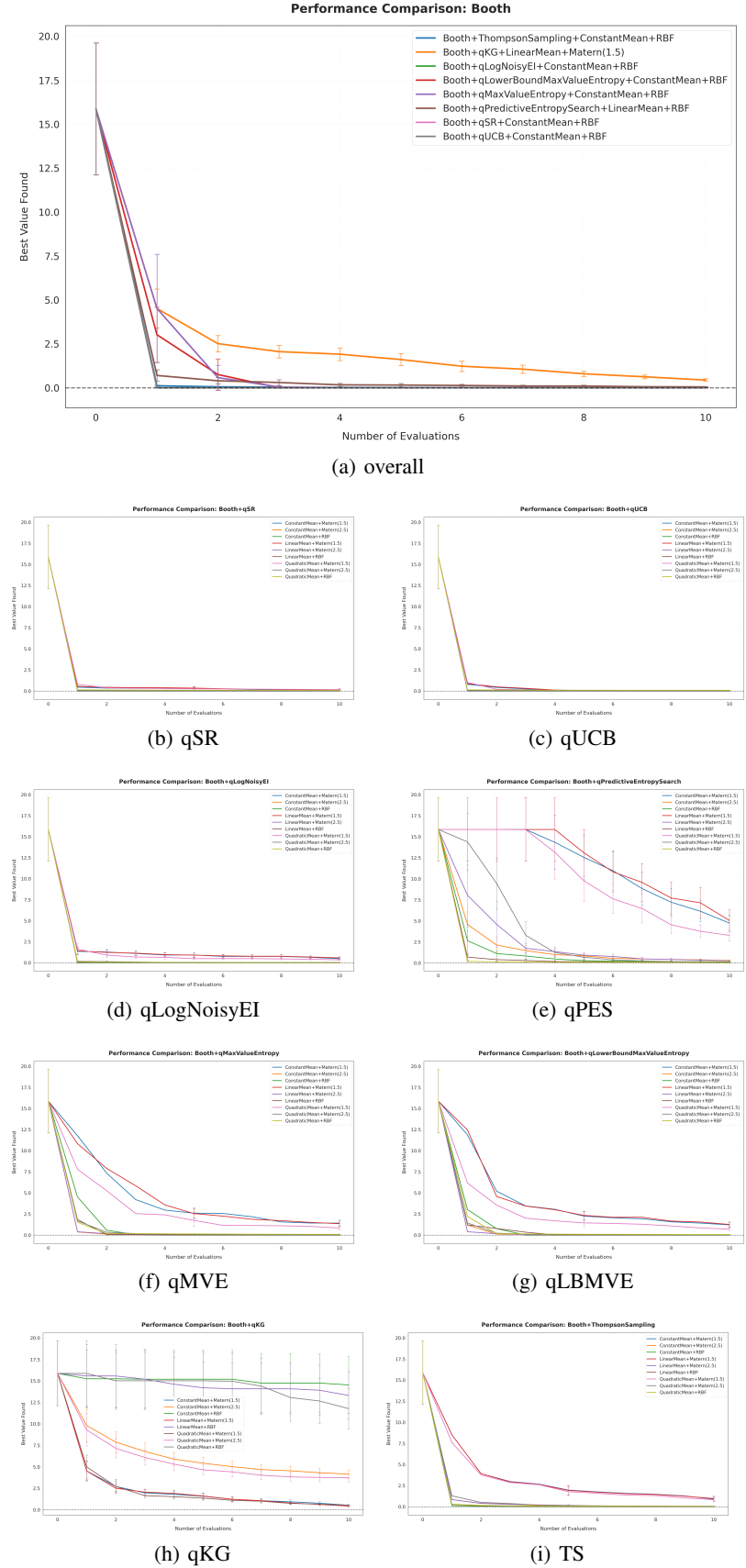


Figure 5: Easom

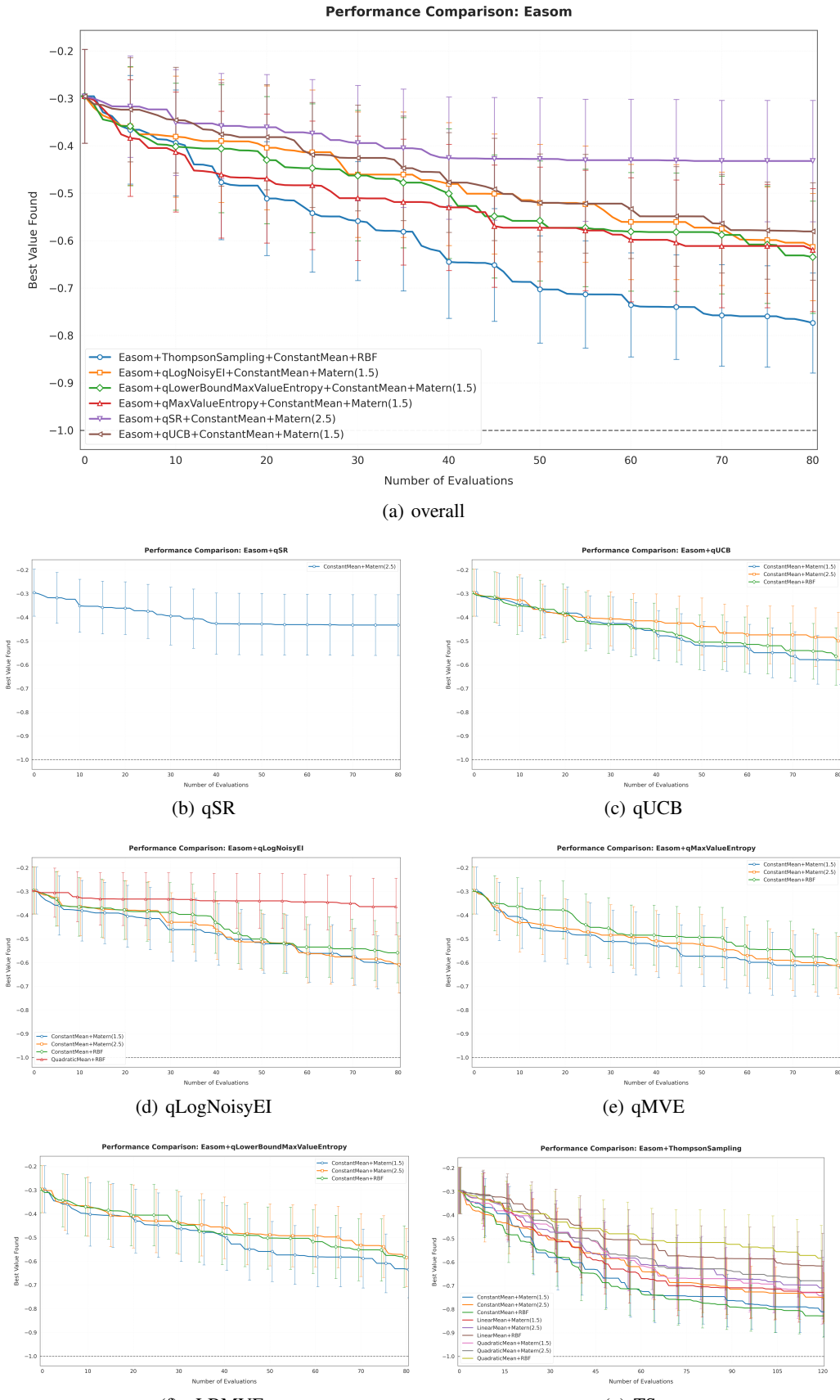
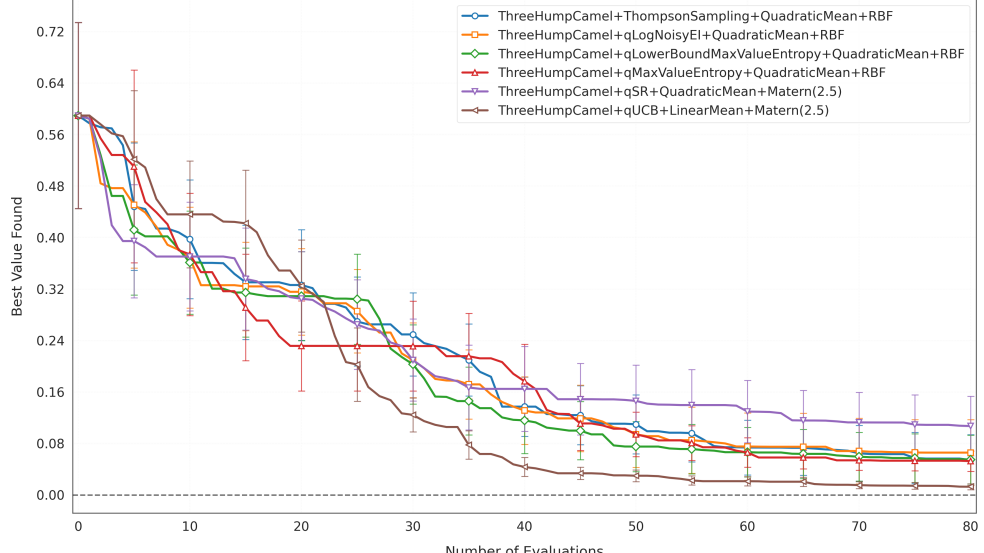
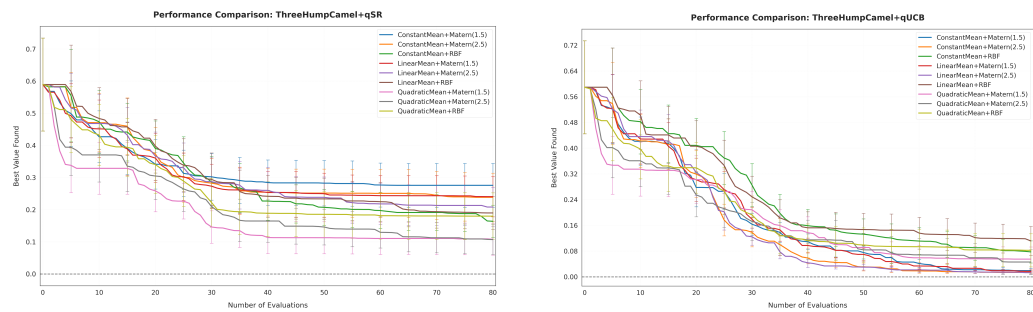


Figure 6: ThreeHumpCamel

**Performance Comparison: Hump Camel**

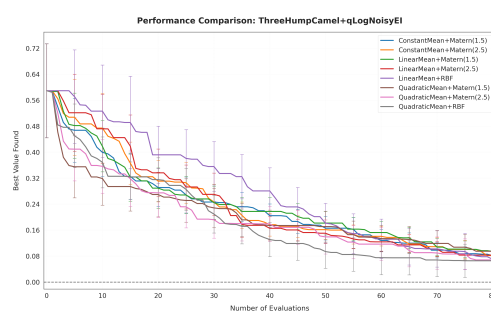


(a) overall

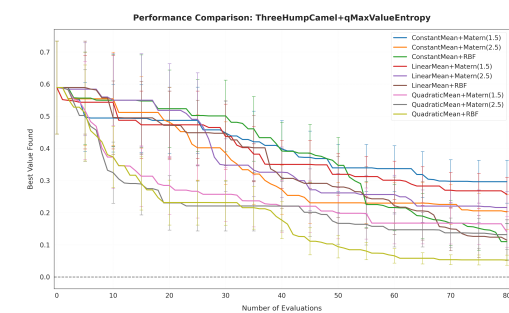


(b) qSR

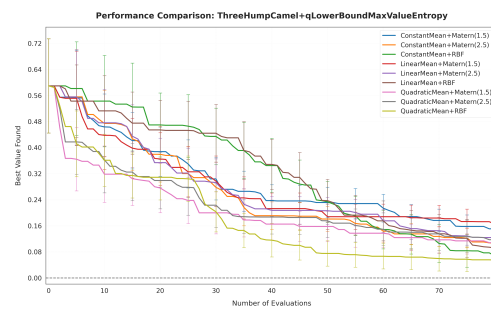
(c) qUCB



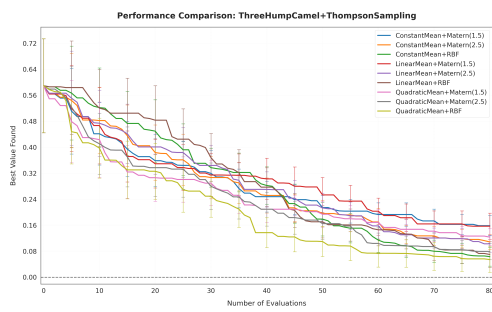
(d) qLogNoisyEI



(e) qMVE



(f) qLBMVE



(g) TS

## 5 Discussion

This study evaluates the performance of various acquisition functions across several benchmark optimization problems, including the Ackley, Bohachevsky, Booth, Easom, and Three-Hump Camel functions. The focus is on understanding how different acquisition strategies perform under varying levels of function complexity and computational constraints.

### Ackley Function

The Ackley function, characterized by its multimodal nature and numerous local optima, poses a significant challenge for optimization algorithms. Among the tested acquisition strategies, qLogNoisyEI, Thompson Sampling (TS), and qLowerBoundMaxValueEntropy (qLBMVE) demonstrated superior performance, consistently converging to low objective values. These methods effectively balance exploration and exploitation, making them suitable for complex, noisy landscapes like Ackley.

In contrast, qSR and qUCB exhibited slower convergence and higher variance, indicating less effective search capabilities in such intricate landscapes. qMaxValueEntropy (qMVE) showed moderate performance, outperforming qSR and qUCB but lagging behind the top-performing methods.

### Bohachevsky and Booth Functions

The Bohachevsky and Booth functions are characterized by simple, convex landscapes. Most acquisition functions achieved near-optimal performance within a limited evaluation budget, with minor differences observed among them. This rapid convergence suggests that optimization tasks on these functions are relatively straightforward and less sensitive to the choice of acquisition function.

However, for the Bohachevsky function, qKG, qMaxValueEntropy (qMVE), qPredictiveEntropy-Search (qPES), and qLowerBoundMaxValueEntropy (qLBMVE), demonstrated relatively poorer performance compared to qLogNoisyEI, TS, qUCB, and qSR. These underperforming methods often rely on complex sampling or entropy-based approximations, which may not be necessary for simple landscapes and can introduce unnecessary computational overhead.

### Easom Function

The Easom function is known for its extremely narrow basin of attraction and a sharp global optimum, making it a particularly difficult target for optimization algorithms. Across all acquisition strategies, most configurations performed poorly, with many failing to produce results. This widespread failure is especially apparent for qSR, likely due to its deterministic and greedy behavior, which fails to explore sufficiently in such a deceptive landscape.

In contrast, Thompson Sampling (TS) emerged as the best-performing acquisition strategy on the Easom function. TS consistently converged closer to the global optimum across all configurations and notably did not fail in any instance. Its stochastic nature enables broader exploration and greater robustness to the function's steep and irregular curvature.

### Three-Hump Camel Function

The Three-Hump Camel function presents a relatively smooth and low-dimensional landscape with moderate complexity. Among all acquisition strategies, qUCB achieved the best performance, consistently converging to near-optimal values faster than others across different configurations. In contrast, qSR exhibited the worst performance, with slow convergence and high variance. The remaining acquisition functions—qLogNoisyEI, qLBMVE, qMVE, and TS—demonstrated comparable performance, showing steady convergence and relatively low variance.

It is important to note that both qKG and qPES were excluded from the comparison on the Ackley, Easom, and Three-Hump Camel functions due to excessive computational costs. These methods failed to return results within the allotted time budget, highlighting their scalability limitations under complex or high-dimensional function evaluations.

## Summary

1. **Overall Performance of Acquisition Functions** The performance of acquisition functions varies depending on the complexity and structure of the objective function. For the Ackley function, which is highly multimodal, acquisition functions like qLogNoisyEI, TS, and qLBMVE achieved better results by effectively balancing exploration and exploitation. In contrast, the Easom function, which has a narrow global optimum and steep curvature, proved challenging for most methods, but Thompson Sampling consistently performed well due to its stochastic nature. For simple convex functions such as Bohachevsky and Booth, most acquisition functions worked adequately, and complex strategies like qPES or qKG offered limited advantage. On moderately complex functions like the Three-Hump Camel, qUCB showed strong performance, while other methods like TS also remained competitive.

- For complex multimodal functions like Ackley, which contain many local optima and require balancing exploration and exploitation, strategies such as qLogNoisyEI, TS, and qLBMVE demonstrated strong performance by effectively navigating the complex landscape.
- For functions like Easom, which are also complex but characterized by a narrow global optimum and steep surrounding curvature, many acquisition functions encountered numerical issues and failed to return valid results. In contrast, Thompson Sampling showed clear advantages—its stochastic nature enables broader exploration and made it more robust and stable under such difficult conditions.
- For simple convex functions (e.g., Bohachevsky, Booth), most acquisition functions performed adequately. In such cases, using computationally expensive strategies like qKG or qPES is often unnecessary.
- For moderately complex functions (e.g., Three-Hump Camel), qUCB achieved the best performance, while other acquisition functions, such as TS, also showed competitive results.

2. **Limitations of qKG and qPES**

qKG and qPES were only included in the comparison for the Bohachevsky and Booth functions due to their high computational costs. Even in these simpler scenarios, their performance was suboptimal compared to other acquisition functions. Their reliance on complex sampling or entropy-based approximations makes them less practical for functions where such sophistication is unnecessary.

3. **Hypotheses regarding the prior mean function**

Our results suggest that the effectiveness of the prior mean function depends on the shape of the objective function. For example, on valley-shaped (e.g., Three-Hump Camel) and bowl-shaped (e.g., Bohachevsky) landscapes, configurations using quadratic mean functions generally performed better. This indicates that aligning the structure of the prior with the geometry of the target function can improve optimization outcomes.

4. **Robustness of Thompson Sampling**

Thompson Sampling (TS) demonstrated remarkable robustness across all tested functions. It consistently performed well and did not encounter any failures or numerical issues. Its stochastic nature allows for effective exploration, making it a reliable choice for a wide range of optimization problems.

These findings underscore the importance of selecting appropriate acquisition functions based on the specific characteristics of the optimization problem at hand. While complex strategies may offer advantages in certain scenarios, simpler methods often provide sufficient performance with reduced computational overhead.

## 6 Conclusion

In this paper, we evaluated eight acquisition functions for single-objective Bayesian optimization under noisy conditions, using a comprehensive experimental design that combined multiple GP model configurations across five representative benchmark functions.

Our findings highlight that **no single acquisition function is universally optimal**. Instead, their performance varies significantly depending on the complexity of the objective function. For simple

convex landscapes, most acquisition functions—regardless of their sophistication—can reach near-optimal performance quickly. In contrast, for more challenging or deceptive functions, acquisition strategies that encourage exploration—such as Thompson Sampling and qLogNoisyExpectedImprovement—tend to perform more reliably.

Notably, Thompson Sampling was the only method that succeeded across all experiments without failure, offering a favorable trade-off between simplicity, robustness, and computational cost. In contrast, qKG and qPES were excluded from most comparisons due to excessive runtime, limiting their practical usability in time-sensitive or complex scenarios.

These results underscore the need to **match acquisition function choice to problem structure and resource constraints**. Simpler methods may suffice for low-dimensional or smooth problems, while more exploratory strategies are essential for noisy or multimodal landscapes.

Future work may extend this analysis to multi-objective settings, explore adaptive model selection, and improve the efficiency of entropy-based methods to enhance their applicability in realistic optimization tasks.

## Appendix A: Summary of Optimization Execution Status Across Scenarios

This section presents a summary of the optimization execution outcomes. The tables below **selectively highlight configurations that encountered execution issues**, including timeouts and failures, during the Bayesian optimization process.

We classify unsuccessful runs into two categories:

- **Timeout:** This indicates that the optimization process was terminated prematurely due to excessive computation time. This situation occurred mainly for **qKG** and **qPES** on more complex objective functions (*Ackley*, *Easom*, and *Three-Hump Camel*), where the computational cost of acquisition function evaluation and optimization was prohibitively high.
- **Fail:** This refers to runtime failures that occurred either:
  1. **During Gaussian Process model updates**, often because the computed covariance matrix was not positive definite. Although BoTorch attempts to resolve such issues by **automatically adding jitter** (a small value added to the diagonal), repeated failure to restore numerical stability results in an exception.
  2. **During acquisition function optimization**, where optimization routines (e.g., L-BFGS-B or Adam) may crash due to malformed acquisition landscapes or numerical instabilities.

These failures are rare but highlight the sensitivity of some acquisition function and model combinations to numerical robustness. All failures and timeouts are explicitly labeled in the tables for transparency and future reproducibility.

Table 4: Execution Summary for Ackley Function (Success, Timeout, and Failures)

Acquisition Function	Kernel	Mean		
		Constant	Linear	Quadratic
<b>qKG</b>	<b>RBF</b>	timeout	timeout	timeout
	<b>Matern(3/2)</b>	timeout	timeout	timeout
	<b>Matern(5/2)</b>	timeout	timeout	timeout
<b>qLogNoisyEI</b>	<b>RBF</b>	complete	complete	fail <sup>2</sup>
	<b>Matern(3/2)</b>	complete	complete	complete
	<b>Matern(5/2)</b>	complete	complete	complete
<b>qPES</b>	<b>RBF</b>	timeout	timeout	timeout
	<b>Matern(3/2)</b>	timeout	timeout	timeout
	<b>Matern(5/2)</b>	timeout	timeout	timeout

Table 5: Execution Summary for Bohachevsky Function (Success, Timeout, and Failures)

Acquisition Function	Kernel	Mean		
		complete	fail <sup>1</sup>	complete
qPES	RBF	complete	fail <sup>1</sup>	complete
	Matern(3/2)	complete	complete	complete
	Matern(5/2)	complete	fail <sup>1</sup>	complete

Table 6: Execution Summary for Booth Function (Success, Timeout, and Failures)

Acquisition Function	Kernel	Mean		
		Constant	Linear	Quadratic
qKG	RBF	complete	complete	timeout
	Matern(3/2)	complete	complete	timeout
	Matern(5/2)	complete	complete	timeout
qPES	RBF	complete	timeout	timeout
	Matern(3/2)	complete	complete	timeout
	Matern(5/2)	complete	timeout	timeout

## Appendix B: Impact of Candidate Set Size on Optimization Stability and Performance

In this section, we examine the effect of varying the **candidate set size**—that is, the number of discretized evaluation points used when computing acquisition function values during Bayesian optimization. This parameter, denoted in our code as `num_candidates`, corresponds to the **batch size of sampled input points** used for **Monte Carlo approximation or maximization** of the acquisition function over the domain. It plays a critical role in acquisition strategies that rely on candidate-based search, especially those using sampling methods or discrete maximization rather than closed-form solutions.

We investigated this effect using three acquisition functions: **qLowerBoundMaxValueEntropy**, **qMaxValueEntropy**, and **Thompson Sampling**. For each method, we conducted experiments with three different candidate set sizes: **500**, **1000**, and **5000**. As shown in Figures 7, 8 and 9, the size of the candidate set directly influenced the stability and quality of optimization results.

Our findings indicate that:

- When using **only 500 candidates**, the optimization outcomes were noticeably unstable, with higher variance across replications and slower convergence.

Table 7: Execution Summary for Three-Hump Camel Function (Success, Timeout, and Failures)

Acquisition Function	Kernel	Mean		
		Constant	Linear	Quadratic
qKG	RBF	timeout	timeout	timeout
	Matern(3/2)	timeout	timeout	timeout
	Matern(5/2)	timeout	timeout	timeout
qLogNoisyEI	RBF	fail <sup>2</sup>	complete	complete
	Matern(3/2)	complete	complete	complete
	Matern(5/2)	complete	complete	complete
qPES	RBF	timeout	timeout	timeout
	Matern(3/2)	timeout	timeout	timeout
	Matern(5/2)	timeout	timeout	timeout

Table 8: Execution Summary for Easom Function (Success, Timeout, and Failures)

Acquisition Function	Kernel	Mean		
		Constant	Linear	Quadratic
qKG	<b>RBF</b>	timeout	timeout	timeout
	<b>Matern(3/2)</b>	timeout	timeout	timeout
	<b>Matern(5/2)</b>	timeout	timeout	timeout
qLBMVE	<b>RBF</b>	complete	fail <sup>1</sup>	fail <sup>1</sup>
	<b>Matern(3/2)</b>	complete	fail <sup>1</sup>	fail <sup>1</sup>
	<b>Matern(5/2)</b>	complete	fail <sup>1</sup>	fail <sup>1</sup>
qLogNoisyEI	<b>RBF</b>	complete	fail <sup>1</sup>	complete
	<b>Matern(3/2)</b>	complete	fail <sup>1</sup>	fail <sup>1</sup>
	<b>Matern(5/2)</b>	complete	fail <sup>1</sup>	fail <sup>1</sup>
qPES	<b>RBF</b>	timeout	timeout	timeout
	<b>Matern(3/2)</b>	timeout	timeout	timeout
	<b>Matern(5/2)</b>	timeout	timeout	timeout
qSR	<b>RBF</b>	fail <sup>2</sup>	fail <sup>2</sup>	fail <sup>2</sup>
	<b>Matern(3/2)</b>	fail <sup>2</sup>	fail <sup>2</sup>	fail <sup>2</sup>
	<b>Matern(5/2)</b>	complete	fail <sup>2</sup>	fail <sup>2</sup>
qUCB	<b>RBF</b>	complete	fail <sup>2</sup>	fail <sup>2</sup>
	<b>Matern(3/2)</b>	complete	fail <sup>1</sup>	fail <sup>1</sup>
	<b>Matern(5/2)</b>	complete	fail <sup>1</sup>	fail <sup>1</sup>

- Increasing the size to **1000 candidates** improved the performance significantly, yielding smoother trajectories and reduced variability.
- The **best results were observed with 5000 candidates**, where both the mean performance and variance were consistently optimal across the three acquisition functions.

These results demonstrate that candidate set resolution is essential for ensuring reliable optimization, particularly in acquisition functions that depend on discrete candidate evaluation, such as entropy-based and sampling-based methods. Based on our experiments, we recommend using at least **1000 candidate points** in practice, especially when working with noisy or multimodal objective functions.

## Appendix C: Effect of Numerical Precision on Optimization Performance

We further investigated how the choice of numerical precision affects optimization outcomes, particularly in the context of Gaussian Process modeling and acquisition function evaluation. In most libraries, including BoTorch and GPyTorch, computations can be performed using either `float32` (single precision) or `float64` (double precision).

Figures [10] and [11] show the performance comparison of Bayesian optimization under two precision settings: `float32` and `float64`. These tests were conducted using Thompson Sampling on the **Ackley** and **Easom** functions, with fixed kernel and mean configurations.

The results reveal that:

- For the **Ackley function** (Figure 10), the difference between `float32` and `float64` was minimal, and both configurations converged to similar objective values with comparable variance. This suggests that for some moderately complex functions, single precision may suffice.
- In contrast, for the **Easom function** (Figure 11), `float64` clearly outperformed `float32`, achieving faster and more stable convergence. This function is characterized by a sharp, narrow global optimum, making it more sensitive to numerical precision.

These findings suggest that the **impact of precision is problem-dependent**. While float32 may be adequate for smooth or well-behaved functions, more numerically challenging functions may benefit from higher precision.

We recommend using float64 when computational resources permit, as it not only improves optimization accuracy in complex landscapes but also helps reduce the likelihood of **numerical instabilities** (e.g., non-positive definite covariance matrices or optimization failures during acquisition maximization), even though it may not eliminate such issues entirely.

## Appendix D: Benchmark Functions

The five benchmark functions selected for this study are as follows:

- **Ackley 2:** Characterized by many local minima, representing highly multi-modal landscapes.  
The mathematical formula is:

$$f(x_1, x_2) = -20 \exp\left(-\frac{1}{5} \sqrt{\frac{1}{2}(x_1^2 + x_2^2)}\right) - \exp\left(\frac{1}{2}(\cos(2\pi x_1) + \cos(2\pi x_2))\right) + 20 + \exp(1) \quad (6)$$

- **Bohachevsky :** A bowl-shaped function with a single global minimum and smooth curvature.  
The mathematical formula is:

$$f(x_1, x_2) = x_1^2 + 2x_2^2 - 0.3 \cos(3\pi x_1) - 0.4 \cos(4\pi x_2) + 0.7 \quad (7)$$

- **Booth:** A plate-shaped function with shallow gradients and a simple global minimum. The mathematical formula is:

$$f(x_1, x_2) = (x_1 + 2x_2 - 7)^2 + (2x_1 + x_2 - 5)^2 \quad (8)$$

- **Easom :** Contains steep ridges and sharp drops, making it difficult for local models to capture global trends. The mathematical formula is:

$$f(x_1, x_2) = -\cos(x_1) \cos(x_2) \exp(-(x_1 - \pi)^2 - (x_2 - \pi)^2) \quad (9)$$

- **Three-Hump Camel:** A valley-shaped function with multiple inflection points and moderate complexity. The mathematical formula is:

$$f(x_1, x_2) = 2x_1^2 - 1.05x_1^4 + \frac{x_1^6}{6} + x_1x_2 + x_2^2 \quad (10)$$

These benchmark functions were chosen to represent a diverse range of optimization landscapes, including multi-modal, bowl-shaped, plate-shaped, rugged, and valley-shaped landscapes. Each function has a unique mathematical form and poses different challenges for optimization algorithms. By evaluating the performance of the acquisition functions on these benchmark functions, we can gain insights into their strengths and weaknesses in different optimization scenarios.

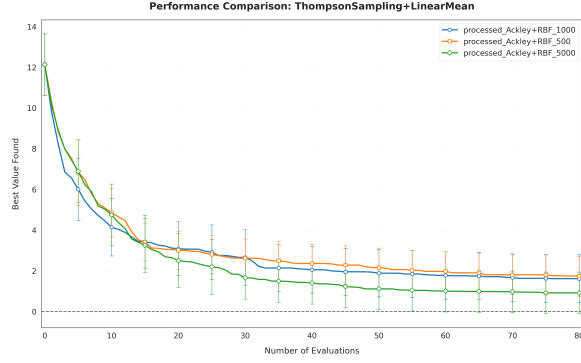


Figure 7: Effect of Candidate Set Size on Thompson Sampling Performance (Linear Mean + RBF Kernel)

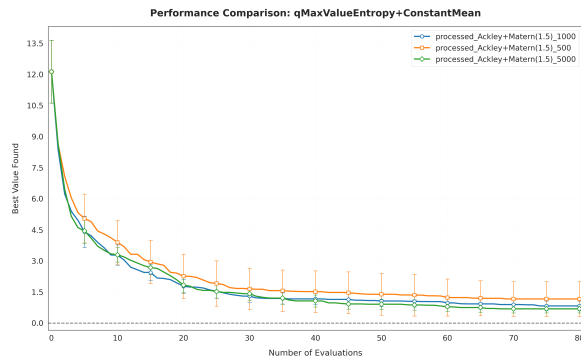


Figure 8: Effect of Candidate Set Size on qMaxValueEntropy Performance (Constant Mean + Matern(1.5) Kernel)

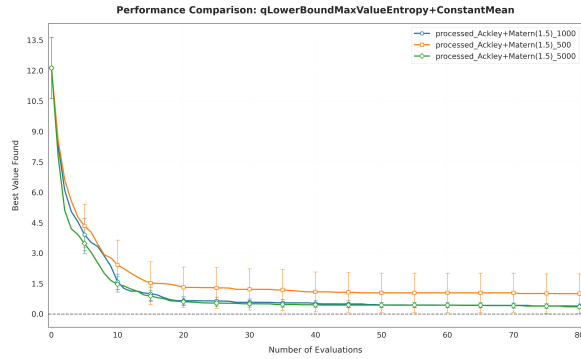


Figure 9: Effect of Candidate Set Size on qLowerBoundMaxValueEntropy Performance (Constant Mean +Matern(1.5) Kernel)

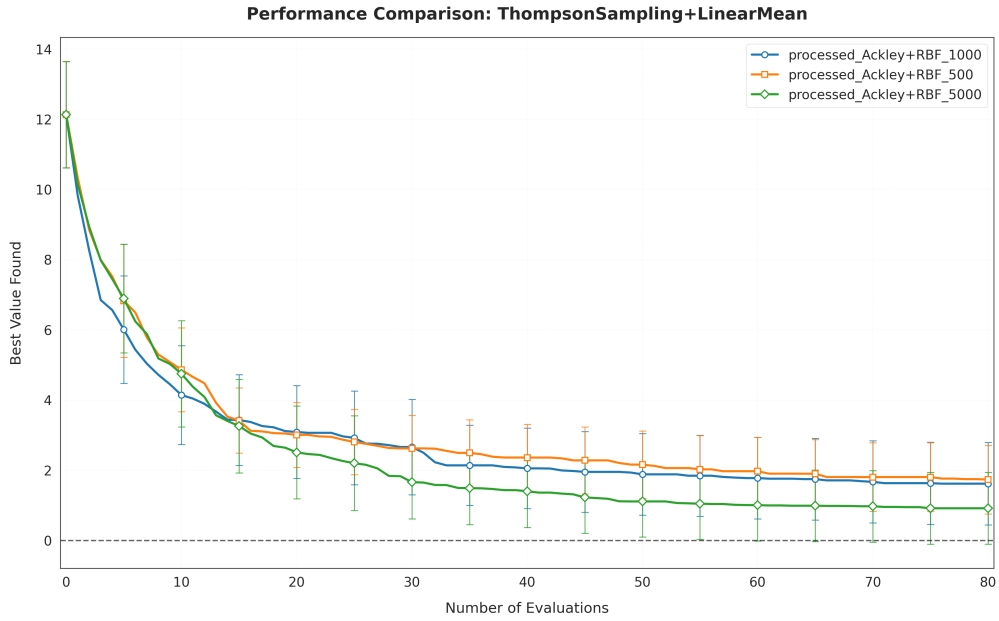


Figure 10: Performance Comparison on Ackley Function using Float32 vs. Float64 Precision(Thompson Sampling + Linear Mean + RBF Kernel)

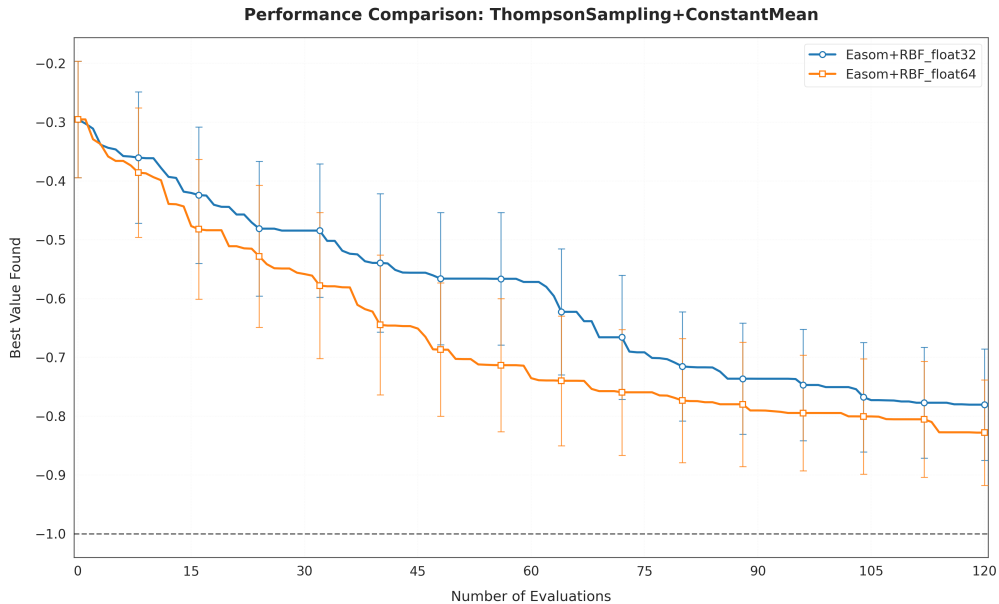


Figure 11: Performance Comparison on Easom Function using Float32 vs. Float64 Precision (Thompson Sampling + Constant Mean + RBF Kernel)

## References

- Maximilian Balandat, Brian Karrer, Daniel R. Jiang, Samuel Daulton, Benjamin Letham, Andrew Gordon Wilson, and Eytan Bakshy. Botorch: Programmable bayesian optimization in pytorch. *CoRR*, abs/1910.06403, 2019. URL <http://arxiv.org/abs/1910.06403>.
- Maximilian Balandat, Brian Karrer, Daniel Jiang, Samuel Daulton, Ben Letham, Andrew G Wilson, and Eytan Bakshy. Botorch: A framework for efficient monte-carlo bayesian optimization. In H. Larochelle, M. Ranzato, R. Hadsell, M.F. Balcan, and H. Lin, editors, *Advances in Neural Information Processing Systems*, volume 33, pages 21524–21538. Curran Associates, Inc., 2020. URL [https://proceedings.neurips.cc/paper\\_files/paper/2020/file/f5b1b89d98b7286673128a5fb112cb9a-Paper.pdf](https://proceedings.neurips.cc/paper_files/paper/2020/file/f5b1b89d98b7286673128a5fb112cb9a-Paper.pdf).
- Peter I. Frazier, Warren B. Powell, and Savas Dayanik. A knowledge-gradient policy for sequential information collection. *SIAM Journal on Control and Optimization*, 47(5):2410–2439, 2008. doi: 10.1137/070693424. URL <https://doi.org/10.1137/070693424>.
- Henry B. Moss, David S. Leslie, Javier Gonzalez, and Paul Rayson. GIBBON: general-purpose information-based bayesian optimisation. *CoRR*, abs/2102.03324, 2021. URL <https://arxiv.org/abs/2102.03324>.
- Bobak Shahriari, Kevin Swersky, Ziyu Wang, Ryan P. Adams, and Nando de Freitas. Taking the human out of the loop: A review of bayesian optimization. *Proceedings of the IEEE*, 104(1): 148–175, 2016. doi: 10.1109/JPROC.2015.2494218.
- WILLIAM R THOMPSON. On the likelihood that one unknown probability exceeds another in view of the evidence of two samples. *Biometrika*, 25(3-4):285–294, 12 1933. ISSN 0006-3444. doi: 10.1093/biomet/25.3-4.285. URL <https://doi.org/10.1093/biomet/25.3-4.285>.
- Zi Wang and Stefanie Jegelka. Max-value entropy search for efficient Bayesian optimization. In Doina Precup and Yee Whye Teh, editors, *Proceedings of the 34th International Conference on Machine Learning*, volume 70 of *Proceedings of Machine Learning Research*, pages 3627–3635. PMLR, 06–11 Aug 2017. URL <https://proceedings.mlr.press/v70/wang17e.html>.
- James T. Wilson, Riccardo Moriconi, Frank Hutter, and Marc Peter Deisenroth. The reparameterization trick for acquisition functions, 2017. URL <https://arxiv.org/abs/1712.00424>.
- Jian Wu and Peter Frazier. The parallel knowledge gradient method for batch bayesian optimization. *Advances in neural information processing systems*, 29, 2016.

Table A1: Performance of Noisy Bayesian Optimization with Different Acquisition Functions on Test Functions

		Ackley (optimal value =0.0)				Bohachevsky (optimal value =0.0)				Booth (optimal value =0.0)				Eason(optimal value =-1.0)				Three Hump Camel (optimal value =0.0)					
		25%	50%	75%	100%	25%	50%	75%	100%	25%	50%	75%	100%	25%	50%	75%	100%	25%	50%	75%	100%		
qSR	Constant	RBF	mean	5.26837386	4.55083874	4.24504532	4.23794638	0.07388865	0.07203123	0.07118676	0.071027684	0.00270056	0.00269863	0.00269129	0.00269129	\	\	\	\	0.39465637	0.22835229	0.19831407	0.16429281
		RBF	var	4.31995981	4.62800259	4.74242971	4.74572882	0.06227427	0.06269046	0.06287388	0.06294359	0.00230954	0.0023088	0.00230641	0.00230641	\	\	\	\	0.25917843	0.1814818	0.16878313	0.15344598
		Matern(3/2)	mean	7.61776305	7.19808256	6.99306265	6.91591094	0.203658638	0.194775669	0.185648393	0.1763975661	0.31391823	0.28179224	0.14167607	0.10938267	\	\	\	\	0.34663137	0.28660712	0.27899417	0.27796217
	Linear	Matern(5/2)	mean	4.41464513	4.64313884	4.71469436	4.74349699	1.55057098	1.54960676	1.5621338	1.535803657	0.6150475	0.56810794	0.21735845	0.20565004	\	\	\	\	0.23371948	0.21445052	0.20806039	0.20728119
		RBF	var	6.12988077	5.58756491	5.3846497	5.23024046	0.11409084	0.06786771	0.05809968	0.05724757	0.0072558	0.00536528	0.00504897	0.00500909	-0.3810611	-0.4493642	-0.4540077	-0.4557483	0.37712446	0.2554956	0.25157343	0.23879742
		Matern(3/2)	mean	4.23729457	4.42516976	4.48045236	4.51724771	0.15759922	0.0921119	0.07565674	0.075110888	0.00735193	0.00554453	0.00534768	0.005363	0.31380832	0.36312361	0.36226766	0.36026979	0.24791799	0.22528316	0.22772362	0.2297595
qUBC	Constant	RBF	mean	5.26496885	5.05634512	4.90423493	4.69366689	0.67917127	0.65541604	0.5858265	0.562732902	0.04509324	0.03864458	0.03567823	0.03021789	\	\	\	\	0.40229399	0.24301422	0.22617636	0.1909988
		Matern(5/2)	mean	4.53651314	4.66425735	4.68602846	4.7483067	0.52663757	0.50739074	0.47174347	0.446711781	0.06868121	0.05319508	0.04207656	0.04207656	\	\	\	\	0.25251805	0.19972384	0.1846204	0.15525908
		Matern(3/2)	mean	8.22954031	7.80448164	7.61740267	7.51784116	1.91617904	1.81529818	0.40062771	0.34276114	0.18605214	0.14623584	0.04062771	0.04062771	\	\	\	\	0.364647	0.2551663	0.24535162	0.24226041
	Linear	Matern(5/2)	mean	4.02199802	5.16358817	4.71917438	4.58390094	0.19076978	0.14794168	0.126960386	0.0191444	0.00860045	0.00660499	0.0065478	0.0065478	\	\	\	\	0.37113734	0.26150819	0.21784012	0.20905414
		Matern(3/2)	mean	4.77110811	4.09864117	4.29799815	4.3504827	0.2210902	0.19910657	0.17941123	0.17072289	0.02152427	0.0142359	0.00935287	0.00937687	\	\	\	\	0.22650497	0.21676745	0.19634652	0.18525515
		RBF	var	5.54073305	5.04937433	4.88953239	4.2843323	3.44E-05	3.31E-05	3.29E-05	0.11325363	0.09753397	0.08930984	0.08802056	0.08802056	\	\	\	\	0.34251625	0.18809477	0.18023277	0.17861555
qLogNoisyEI	Constant	Matern(5/2)	mean	5.13720049	6.59329471	6.19481573	5.77357812	3.42E-05	3.29E-05	3.26E-05	0.01821512	0.012209	0.0109002	0.00996584	0.00996584	\	\	\	\	0.30740748	0.16377675	0.13903475	0.10605489
		Matern(3/2)	mean	2.92450388	2.91680498	2.77733057	3.13112929	3.89E-05	3.87E-05	3.85E-05	0.01965029	0.01840506	0.01834404	0.01834404	0.01834404	\	\	\	\	0.22211489	0.20015449	0.14757956	0.14063753
		RBF	var	3.69429923	2.73040959	1.99803053	1.78633556	0.05625904	0.05189536	0.04942978	0.048653296	0.0021678	0.0014411	0.00124059	0.00123988	-0.4041812	-0.4797065	-0.5387429	-0.5913407	0.41346750	0.15911521	0.11064719	0.07663301
	Linear	Matern(5/2)	mean	4.22757569	4.04010858	4.08099353	1.76529213	1.0303309	0.49353457	0.43992482	0.28330402	0.06747375	0.0535763	0.02012166	0.31065486	0.28624532	0.27854788	0.26909758	0.18160733	0.07327746	0.03796591	0.02259397	0.02259397
		Matern(3/2)	mean	3.99678055	2.60405478	2.23954828	2.11755582	0.21520765	0.18131885	0.10730003	0.09882968	0.08036177	0.00533602	0.00513424	0.0050025	-0.4124415	-0.4387298	-0.4978437	-0.5204845	0.03231801	0.05862621	0.01842321	0.01356631
		RBF	var	4.02168532	3.94523871	3.48639222	3.5191206	0.21725476	0.14341335	0.10953429	0.102483438	0.01172101	0.00695137	0.00676378	0.00659046	0.31068326	0.32406121	0.33728462	0.33456339	0.22194465	0.05508884	0.0217861	0.01415446
qPredictiveEntropySearch	Constant	Matern(5/2)	mean	4.04132923	3.45238781	3.48639222	3.5191206	0.21725476	0.14341335	0.10953429	0.102483438	0.01172101	0.00695137	0.00676378	0.00659046	0.31068326	0.32406121	0.33728462	0.33456339	0.22194465	0.05508884	0.0217861	0.01415446
		Matern(3/2)	mean	4.47007994	3.93142889	3.98544189	4.01505356	0.54336325	0.54584574	0.48098984	0.45482064	0.06748525	0.05381269	0.04951884	0.04629756	\	\	\	\	0.3042878	0.09823593	0.03372444	0.01679456
		RBF	var	5.88996866	5.04089041	4.74124727	4.29268633	0.20739939	1.76698526	1.1675894	1.11706163	0.32052031	0.0784246	0.04861324	0.02179025	\	\	\	\	0.23082845	0.07057911	0.03002188	0.01379191
	Linear	Matern(5/2)	mean	4.68844344	4.81897891	4.7759495	4.71515884	0.17745032	1.4588936	0.54509002	0.490341326	0.31634068	0.07896841	0.06182163	0.02179025	\	\	\	\	0.32811637	0.03		